Nitrogen retention and ammonia production on tungsten

Florin Ghiorghiu, T. Aissou, Marco Minissale, Thierry Angot, G. de Temmerman, Régis Bisson

Nitrogen Retention and Ammonia Production on Tungsten

F. Ghiorghiu[1], T. Aissou[1], M. Minissale[1], T. Angot[1], G. De Temmerman[2,3,4], R. Bisson[1,*]

[1]Aix-Marseille Univ, CNRS, PIIM, UMR 7345, Marseille, France

[2] ITER Organization, St. Paul Lez Durance Cedex, France

[3] Zenon Research, F-75006 Paris, France

[4] MINES ParisTech, University PSL, Institute of Higher Studies for Innovation and Entrepreneurship (IHEIE), 75006 Paris, France

[*] Email: regis.bisson@univ-amu.fr

Abstract. We report a systematic study that quantifies nitrogen retention and ammonia production on tungsten and that sheds light on the mechanism for ammonia formation on ITER's divertor material. Saturation of the nitrogen-implanted layer in polycrystalline tungsten is observed at room temperature for a nitrogen ion fluence in the low 10^{21} N^+ m^{-2} range. Nitrogen desorption from this N-implanted layer occurs in the 800 – 1100 K temperature range and exhibits a zero-order kinetics with an activation energy of 1.45 eV and a prefactor of 5×10^{24} m^{-2} s^{-1}. Following nitrogen and deuterium co-implantation, deuterated ammonia production is observed during temperature programmed desorption between 350 K and 650 K in conjunction with deuterium desorption. In contrast, nitrogen desorption still occurs above 800 K. Significant production of ammonia is obtained only when the nitrogen layer created by ion implantation is approaching saturation and the amount of nitrogen lost to ammonia production is only in the percent range. This result is understood by repeating cycles of deuterium implantation and thermo-desorption below the desorption temperature of the nitrogen layer. The exponential decay of the amount of produced ammonia with cycle number demonstrates that nitrogen diffusion to the surface is negligible in the ammonia production temperature range and that ammonia formation occurs at the outermost surface layer. The maximum quantity of ammonia produced from the present N implanted layer is below 2×10^{18} ND_3 m^{-2}, which is limited by the nitrogen atom surface density. Surface vibrational spectroscopy demonstrates the presence of ammonia precursors on the nitrogen-implanted tungsten surface upon deuterium implantation. These ammonia precursors can be created also at room temperature through the dissociative chemisorption of thermal D_2 catalyzed by nitrogen present at the tungsten surface and, more efficiently, by adsorption of deuterium atoms.

1. INTRODUCTION

For high-power operations in ITER, it is foreseen to inject extrinsic impurities into the edge plasma to dissipate part of the plasma exhaust power through radiation and maintain the power fluxes to the plasma-facing components (PFCs) within tolerable limits (10 MW m^{-2}) [1]. To date, the best compromise between radiative efficiency [2] and hot plasma performance [3, 4] has been achieved with the injection of molecular nitrogen in the edge plasma region. However, injection of nitrogen (N) in a divertor plasma environment next to metallic components leads to a significant conversion of the injected nitrogen into ammonia (NH_3) [5, 6], although the first experimental estimations of the conversion fraction (~10%) are still subject to some uncertainties [7]. In ITER, ammonia production will be concurrent with a deuterium/tritium plasma thus radioactive tritiated ammonia is expected.

The formation of large amounts of tritiated ammonia has consequences for several aspects of the ITER plant operation in terms of tritium retention, gas reprocessing and duty cycle. It is well known that ammonia is a polar molecule and could stick on shadowed metallic in-vessel components as well as on pumping ducts. This represents an issue for the tritium recycling plant operated to retrieve tritium from cryopumps and exhaust gases. Recently, using molecular beam techniques, we have reported the absolute sticking probability of NH_3 on tungsten (W) and stainless steel 316-L surfaces as they will be used in ITER, i.e. covered with natural impurities such as carbon and oxygen. We were able to reproduce our well-controlled experiments with a Generalized and Separable Kisliuk kinetic model that can be used to forecast the coverage of NH_3 on W and 316-L surfaces as a function of the surface temperature and the ammonia flux [8].

However, it is currently unclear how and where NH_3 formation predominantly occurs in fusion devices, which makes it difficult to predict the ammonia formation rate in ITER and thus the ammonia flux expected on areas in the vacuum vessel where ammonia might accumulate. While significant NH_3 formation was reported in ASDEX Upgrade [5] and JET [6] tokamaks during N-seeded discharge, recent experiments in the full-W tokamak WEST [9] evidenced an absence of ammonia formation concurrent with PFCs that are still able to pump nitrogen. This result in WEST suggests that the N wall reservoir must be saturated in order to produce ammonia in significant amounts.

Laboratory studies on the saturation of nitrogen retention in wall materials, such as tungsten, are rather sparse. Meisl *et al.* [10] have shown using X-ray photoelectron spectroscopy (XPS) and nuclear reaction analysis (NRA) that nitrogen ion implantation at room temperature with 45° incidence angle and 2.5 keV/N (respectively, 500 eV/N) leads to nitrogen retention saturation of 2.3×10^{20} N m^{-2} (1.1×10^{20} N m^{-2}). Thus, there is an apparent influence of the incident kinetic energy of N species on the saturation of the nitrogen layer, that Meisl *et al.* attributed to a negligible diffusion of nitrogen in W up to 800 K. This negligible diffusion of N in W between 300 K and 800 K has been confirmed by measurements of the N bulk profile with a combination of XPS and Ar sputter depth profiling as a function of N implantation temperature in the work of Plank *et al.* [11]. Ogorodnikova *et al.* [12] measured with NRA that N-seeded ($\leq$ 5%) deuterium (D) plasma exposure at 300 K and normal incidence and with 30 – 100 eV/N gives a nitrogen retention saturation in the $0.7 – 0.9\times10^{20}$ N m^{-2} range. This relatively high retention, considering the low implantation kinetic energy, has been rationalized by Meisl *et al.* as the results of recoil implantation of nitrogen by deuterium in N-seeded D plasma [10]. However, these quantitative works reported on the retention of nitrogen but not on the production of ammonia molecules. Instead, they discussed the subsequent N erosion [10] and D retention [12, 13].

Laboratory studies on the production of ammonia from tungsten has been so far realized with plasma discharges in the 10^{-4} - 10^{-2} mbar pressure range. De Castro *et al.* used mass spectrometry to follow the consumption of nitrogen and the production of ammonia in N+H plasma glow discharges and observed an incubation time for obtaining an enhanced ammonia production yield [14]. This result was interpreted as the need for the N metallic wall reservoir to be saturated, consistent with the further observation that firstly a N plasma wall loading was needed to produce deuterated ammonia during a subsequent D plasma exposure [15]. However, Laguardia *et al.* used mass spectrometry and chromatography to show that the ammonia yield was also dependent on plasma parameters such as total pressure and electron energy in their linear plasma device [16]. Yaala et al. finally demonstrated that, in addition to ammonia production in the plasma, ammonia production is catalyzed by tungsten walls indeed, by comparing N+H plasma discharges in a quartz tube and in a quartz tube containing a tungsten foil in the after-glow [17, 18]. In summary, these plasma laboratory studies showed that W walls act as a N reservoir which impacts the formation of ammonia through plasma-surface interactions, consistently with observations in tokamaks [5, 6, 9]. However, a mechanistically-informed quantitative estimate of how much ammonia can be produced from

tungsten materials exposed to nitrogen and deuterium species is still missing. Ion beam experiments performed in ultra-high vacuum conditions are therefore needed to achieve this goal.

In the present work, we performed a systematic and quantitative study of the production of deuterated ammonia (ND_3) from polycrystalline W samples co-implanted sequentially with N and D ions. In Section 2, we describe the experimental setup and the methodology used to (co-)implant N and D in tungsten and to measure the production of ND_3 during thermo-desorption experiments. In Section 3.1, we present our results on the retention of nitrogen in polycrystalline W and on the saturation of a nitrogen-implanted tungsten layer. We then show and discuss the temperature programmed desorption behaviour of nitrogen implanted in W. In Section 3.2, we evidence the production of deuterated ammonia from nitrogen and deuterium co-implanted in tungsten upon thermo-desorption and we present a quantitative analysis of this ND_3 production as a function of deuterium fluence. In Section 3.3, we highlight a limiting factor for ND_3 production, we show the vibrational signature of the ammonia surface precursor and we discuss the resulting interpretation in terms of ammonia formation mechanism. This paper ends on a summary and on a perspective on future studies that could contribute further to the estimation of the tritium inventory from tritiated ammonia in ITER.

2. EXPERIMENTAL METHODS

Tungsten PFCs in ITER are made of polycrystalline tungsten with specific grain elongation to avoid the formation of cracks parallel to the surface [19]. However, in our experimental approach we use model samples which can withstand multiple implantations and thermo-desorption cycles without structure evolution that could affect either their deuterium retention or their thermal release of molecules containing hydrogen isotopes [20–22]. Therefore, we used recrystallized and mirror-like mechanically and electro-polished polycrystalline W samples from A.L.M.T. Corp. (Japan) with 99.99 wt.% purity and with dimensions of $10\times10\times0.4$ mm^3. Two W samples from the same batch were used in this study, giving identical results, and thus the two samples data were used in the following for calculations of the mean and the standard deviation of replicate measurements.

Most experiments were conducted in the CAMITER set-up [22] located at PIIM laboratory (Aix-Marseille University – CNRS). The experimental apparatus consists in two

interconnected ultra-high vacuum (UHV) chambers: a differentially-pumped load-lock/storage chamber (base pressure < 3×10^{-9} mbar) and an implantation/temperature programmed desorption (TPD) chamber (base pressure < 2×10^{-9} mbar). The implantation/TPD chamber is equipped with an OMICRON ISE 10 ion source, a PID/thermocouple-controlled radiative (tungsten filament) oven and a differentially-pumped chamber (base pressure < 1×10^{-10} mbar) containing the quadrupole mass spectrometer (HIDEN 3F/PIC, noted QMS in the following) which is located in a line-of-sight 2 mm above the sample. An all-metal leak valve connected to the ion source controls the D_2 or N_2 gas flow. The majority ion species (>95%) are D_2^+ or N_2^+ ions, as verified with a quadrupole mass filter analyser (Hiden EQP), and they are accelerated to a kinetic energy of 500 eV. Thus, the majority of ion fragments passing the surface are assumed to have a kinetic energy of 250 eV per nucleus and a small fraction of atomic ions should be at 500 eV per nucleus. Ions impinge the sample with an incidence angle of 45° through a collimating pinhole defining an elliptical projected area of 0.5 cm^2. The implantation range of the ensuing 250eV D and N fragments are estimated with the binary collision code SRIM [23] to be ~4 nm and ~1 nm, respectively. A single ion source has been used to ensure an optimal overlap of the two ion beams footprints on the W sample. Thus, a thorough pumping/degassing of the ion source is performed after each switching of the gas feed, with the W sample located in the load-lock/storage chamber. To transfer samples between UHV chambers, tungsten samples are mounted on a molybdenum flag-style sample plate. The ion flux is determined by measuring the current on the sample with a picoammeter (Keithley 410A). The total incident fluence is calculated by converting the sample current into particle flux and by multiplying the particle flux with the duration of the implantation. We did not correct the measured sample current from secondary electron emission since we observed that, for a given ion source condition, the sample current did not vary more than 20%, the usual day-to-day fluctuation, when comparing implantation of D in pristine W and in N-implanted W. Secondary electron emission resulting from D_2^+ and N_2^+ ions are unknown in our experimental conditions and it has been reported to be less than 10% for 1 keV Ar^+ in Plank et al. [11]. Thus, secondary electron emission is likely a small correction on the fluences reported here.

Once W samples were introduced in the load-lock/storage chamber from air, they were subjected to a degassing procedure consisting of at least two linear temperature ramps of 1 K s^{-1} up to 1300 K followed by a 10 min annealing at 1300 K. This procedure removes most of

hydrocarbons impurities and leaves a native tungsten oxide on the surface [21]. A sequential co-implantation/TPD experiment consists in first implanting the W sample with N ions at a constant flux of ~ 1×10^{16} N^+ m^{-2} s^{-1} for a determined duration to obtain the desired N fluence. After a thorough ion source degassing, the N-implanted W sample is bombarded with D ions at a constant flux of ~ 1.6×10^{16} D^+ m^{-2} s^{-1} for a given duration to reach the desired D fluence. The sample is then transferred to the load-lock/storage chamber in order to degas the oven on which the sample was mounted during implantation. Indeed, during N (D) ion implantation a significant neutral N_2 (D_2) flux is also present, which dissociates and adsorbs on the oven assembly. Once the oven is nitrogen and deuterium-free and cooled down to room temperature (typically after 2 hours), the sample is finally inserted on top of the oven and the TPD is performed. During TPD, the sample temperature is increased linearly with a ramp of 1 K s^{-1} and its value is recorded simultaneously with the desorption rates measured by the multiplexed QMS at m/z = 3, 4, 14, 15, 16, 17, 18, 19, 20 and 28.

Usually, D retention is determined through time integration of the desorption rate of deuterium- containing molecules (m/z=3, 4 and 20 for, respectively, HD, D_2 and ND_3) during the TPD. Our method for conversion of the QMS signals into desorption rates from the sample has been detailed for HD and D_2 and has been checked with Nuclear Reaction Analysis (NRA) in [20]. In the present paper, we will not discuss the D retention in N co-implanted W but focus instead on N retention and ND_3 production. Nitrogen retention is calibrated in a similar way than D retention, i.e. using an off-axis leak valve in the implantation chamber to create a known flux of N_2 entering the differential stage of the QMS [20]. To record the nitrogen desorption rate we used m/z=14 instead of m/z=28, the latter being perturbed by the concomitant emission of CO molecules from the hot oven. We have checked with Auger Electron Spectroscopy in the AMU-PSI setup located at PIIM laboratory (Aix-Marseille University – CNRS) [8], equipped with the same ions source than CAMITER, that all N is desorbed after the TPD (not shown), thus the present TPD measurements are appropriate to determine N retention. Note that we included also the contribution from ND_3 at m/z=20 for the N retention. Finally, deuterated ammonia production is evaluated using solely m/z=20, since NHD_2 (m/z=19) and NH_2D (m/z=18) products are overwhelmed with, respectively, the fluorine background from the QMS ionization head and the water background from the UHV chamber. Thus, deuterated ammonia production reported in this work are to be considered as lower limits. For the calibration of ND_3 production we used the calibration realized for D and N retention corrected from relative partial ionization cross

sections at the ionizing energy of 50 eV [24, 25]. We did not use off-axis leak valve calibration for ND_3 because the CAMITER set-up is not designed to handle a significant pressure of corrosive ammonia as needed for the calibration procedure. We checked that a correction based on partial ionization cross sections was accurate for a variety of gases (H_2, D_2, He, CH_4, Ne, N_2 and Ar). We stress that the line-of-sight geometry of the present TDS set-up minimizes disturbances on partial pressure measurements related to multiple adsorption/desorption of ND_3 on the apparatus metallic walls, in contrast to a QMS installed in a non-line-of-sight geometry [8].

Finally, a third W sample from the same batch was (co-)implanted with N and D ions thanks to an identical ion source in the NAUTILUS set-up [26] located at PIIM laboratory (Aix-Marseille University – CNRS). This multi-chambers UHV setup (base pressure < 2×10^{-10} mbar) is equipped with an OMICRON ISE 10 ion source, a OMICRON EFM-H deuterium atom source based on a hot (>2500 K) W capillary [27, 28], a home-made radiative oven and a VSI DELTA 0.5 high-resolution electron energy loss spectrometer (HREELS) allowing to record the vibrational spectrum of adsorbates present at the surface of the (co-) implanted W sample.

3. RESULTS AND DISCUSSION

3.1. Nitrogen retention in polycrystalline tungsten: the saturation of the nitrogen-implanted tungsten layer and its desorption

Figure 1 presents the evolution of the nitrogen retention in polycrystalline tungsten as a function of the nitrogen ion fluence implanted at room temperature. As the nitrogen fluence is increased from 0.1×10^{20} N^+ m^{-2} to 4.5×10^{20} N^+ m^{-2}, the nitrogen retention increases sublinearly ($\propto$fluence$^{0.80\pm0.05}$) indicating a quite negligible nitrogen diffusion in tungsten at the implantation temperature of 309±8 K and resulting in an apparent implantation probability of about 10 %. Then, the nitrogen retention saturates at a value of $4.2\pm1.1\times10^{19}$ N m^{-2}. The nitrogen fluence necessary to achieve the saturation of N retention is comprised between 4.5×10^{20} N^+ m^{-2} and 1.1×10^{21} N^+ m^{-2}.

The present results obtained by integration of TPD experiments are consistent with the work of Meisl *et al.* [10] and Ogorodnikova *et al.* [12] within a factor of two, despite the use of different quantification methods. Meisl *et al.* showed with X-ray photoelectron spectroscopy

and NRA quantification of N retention, that room temperature implantation of 2500 eV/N and 500 eV/N ions resulted in a saturation of the N retention to values of 2.3×10^{20} N m^{-2} and 1.1×10^{20} N m^{-2}, respectively, for an ion fluence above ~1×10^{21} N^+ m^{-2} and ~6×10^{20} N^+ m^{-2}, respectively. Considering that in the present study the kinetic energy per nitrogen nucleus is further reduced to 250 eV/N, the measured (by TPD) reduction of the saturation of N retention to $0.4\pm0.1\times10^{20}$ N m^{-2} confirms that nitrogen diffusion is negligible at room temperature and thus saturation of retention is the result of a balance between the depth profile of N implantation and the erosion of implanted nitrogen through physical sputtering. We note that the binary collision code SRIM [23] shows, consistently, a reduction by a factor of three of the implantation range (from ~3 nm to ~1 nm) when N ions impinging a W sample at an angle of 45° have their incident energy reduced from 2500 eV to 250 eV. Finally, our saturation of the retention at $0.4\pm0.1\times10^{20}$ N m^{-2} for 250 eV/N ions is also consistent with Ogorodnikova *et al.* who measured a retention of $0.7\text{-}0.9\times10^{20}$ N m^{-2} for 100 eV/N simultaneously co-implanted ions, that would correspond to a retention < 0.4×10^{20} N m^{-2} once corrected for co-implantation recoil [10].

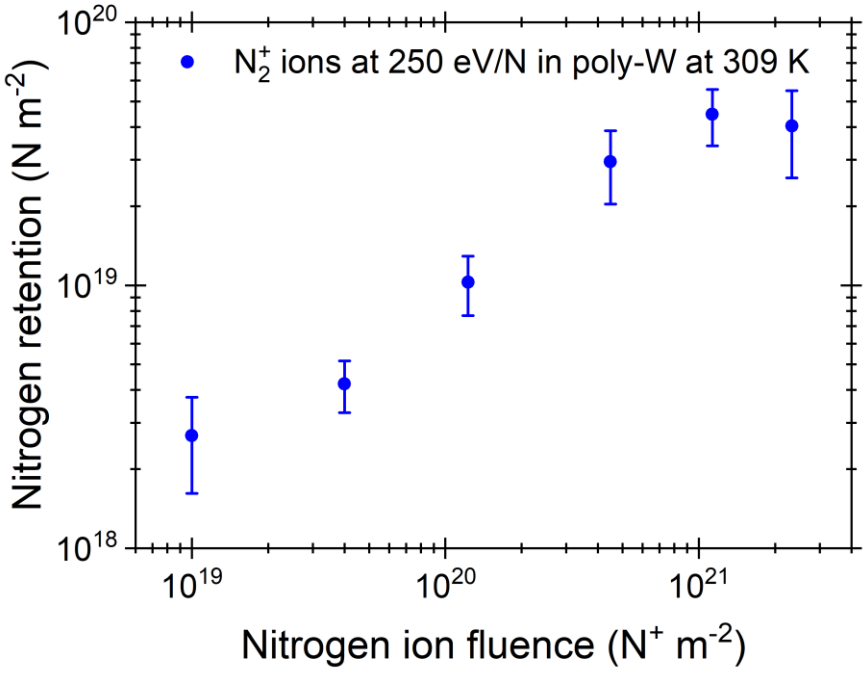

Figure 1. Evolution of the nitrogen retention in tungsten as a function of nitrogen ion fluence. All data points are the average of at least two measurements. Error bars are ±σ from replicate measurements.

Figure 2 shows some selected temperature programmed desorption of the nitrogen-implanted tungsten layers used for figure 1. The onset of nitrogen release in the form of N_2 molecules is observed at 800 K. The nitrogen release rate increases with the surface temperature until it suddenly drops to zero. The temperature at which the nitrogen desorption rate starts to drop, i.e. the peak position, increases with the N content of the N-implanted W layer and reaches 1100 K for a saturated N layer. A TPD series with varied fluence which have a common rising leading edge on the low temperature tail followed by a sharp dropping trailing edge that shifts to higher temperature with increasing fluence is the typical signature of a zero-order desorption i.e. a desorption that is independent of the density of the desorbing species. Such peculiar TPD behaviour is commonly observed in the desorption of condensed multilayers, i.e. the sublimation of atomic and molecular solids [29], or the decomposition of a binary compounds such as WO_2 [30]. Using the sparse thermodynamic data available on the N-W system, Schmid *et al.* [31] argued that the stable phase formed at room temperature for nitrogen implanted in W would be WN and that it should be stable up to a temperature of ~600 K because nitrogen diffusivity is negligible. Such negligible diffusivity has been confirmed by the XPS data of Meisl *et al.* [10] and Plank *et al.* [11] up to 800 K. Above 600 K (in Schmid *et al.* model) or 800 K (according to Meisl *et al.* et Plank *et al.* experiments), the WN layer is expected to decompose since it is not a thermodynamically stable phase. Considering that our TPD is performed at 1 $K.s^{-1}$, i.e. in a quasi-equilibrium condition, one can consider the observation of a zero-order desorption kinetics as the results of an equilibrium between two coexisting phases, a dense and a dilute phase [32], i.e. the decomposing dense nitrogen phase WN layer and the dilute nitrogen desorbing phase at the W surface. For this equilibrium to be maintained over the course of the thermo-desorption, diffusion of nitrogen to the surface should be fast with respect to the desorption rate. In those conditions, the desorption rate of nitrogen would only depend on the sample temperature, i.e. it would be independent of the nitrogen density in the decomposing WN layer, and zero-order desorption would be observed like in Figure 2. Since in a zero-order kinetics the desorption rate has the simple form of the Arrhenius equation $\nu \times \exp(-E_a/kT)$, one can easily extract the kinetic parameters for the activation energy E_a and the prefactor ν thanks to an Arrhenius plot. Such analysis has been realized and the result is used in figure 2 to illustrate how the set of parameters $E_a=1.45\pm0.03$ eV and $\nu=5\pm1\times10^{24}$ m^{-2} s^{-1} correctly reproduces the experimental measurements of the common rising leading edge of the nitrogen desorption peak.

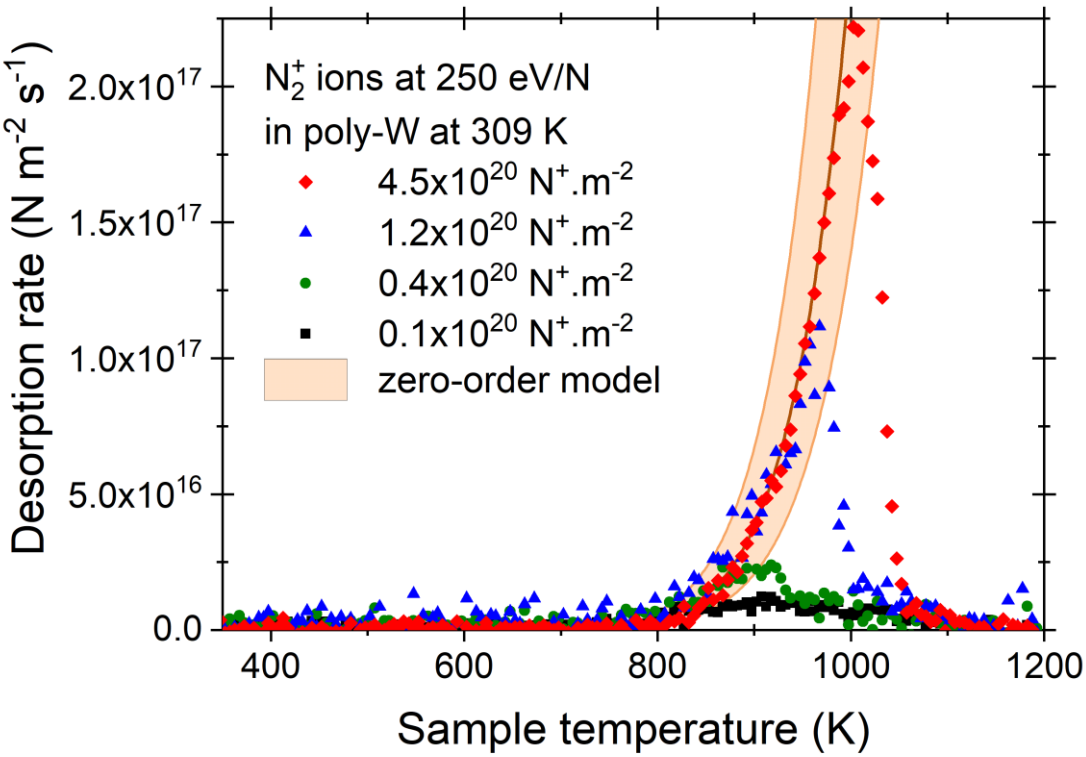

Figure 2. Comparison of TPD measurements obtained for four different nitrogen ions fluence implanted at room temperature. The QMS signal is recorded at m/z=14 to avoid the detection of CO desorption from the oven at m/z=28. The zero-order desorption kinetic model uses the following Arrhenius parameters: E_a=1.45±0.03 eV and ν=5±1×10^{24} m^{-2} s^{-1}.

To summarize the present results on polycrystalline W, we obtained a saturated nitrogen layer containing about 4×10^{19} N m^{-2} by N ion implantation at 45° and 250 eV/N. Note that these values have been obtained for N ions implanted at 309 K, but lower nitrogen content should be obtained for N ions implanted at higher temperature as shown by Plank *et al.* [11]. The obtained nitrogen layer is stable up to 800 K, where it finally desorbs within the temperature range of 800 – 1100 K with zero-order kinetics typical of an unstable WN compound decomposition with fast N diffusion to the surface and an activation energy for nitrogen desorption of E_a=1.45±0.03 eV. These results are consistent with several recent works on WN_x layers that are now discussed.

For polycrystalline W, Meisl *et al.* [10] used N ion implantation at 45° incidence and 2.5 keV/N to produce a saturated nitrogen layer containing 2.3×10^{20} N m^{-2}. With X-ray photoelectron spectroscopy, they observed that nitrogen did not diffuse up to 800 K. Then

between 900 and 970 K a loss of nitrogen was observed, however, the loss was not complete at their maximum heating temperature of 970 K. For similar polycrystalline samples, Ogorodnikova *et al.* [12] used N-seeded D plasma exposure with normal incidence and 100 eV/N to produce nitrogen layers with 7-9×10^{19} N m^{-2}, as determined by NRA. They, found with TPD that nitrogen release was complete at 1200 K. However, the shape of the TPD peak is quite difficult to assess in this publication and there were no systematic studies of the effect of nitrogen fluence onto N thermo-desorption. Nevertheless, these two publications agree with the present results (within the usual absolute uncertainty of the sample temperature measurements) as it appears that nitrogen mobility sets in between 800 and 900 K and that complete desorption of nitrogen is observed between 1100 and 1200 K

For W coatings deposited on a Si substrate, Mateus *et al.* [33] studied the thermal stability of W_2N with elastic backscattering spectroscopy and observed that nitrogen was partially lost between 873 K and 1073 K. Gao *et al.* [13] performed TPD onto a magnetron-sputtered tungsten nitride WN_x thin-film and observed the onset of N_2 release at 830 K with a full desorption occurring at 970 K occurring in two stages, the last stage being reminiscent of the sharp dropping trailing edge that we observed in the present study.

Therefore, even though there are differences by about 100 K in the onset and the termination of nitrogen desorption in all these W-N phases of different stoichiometry, the sample temperature range of 800 – 1200 K appears to be a common window for decomposition of WN_x layers.

3.2. Deuterated ammonia production from polycrystalline tungsten sequentially co-implanted with nitrogen and deuterium

3.2.1. Identification of deuterated ammonia production

Prior to study the production of ND_3, we have performed a series of control experiments dedicated to confirm that the signal observed at m/z=20 originates from deuterated ammonia and not, for example, deuterated water that could be created subsequently to D implantation because of the native oxide present on the tungsten surface [21].

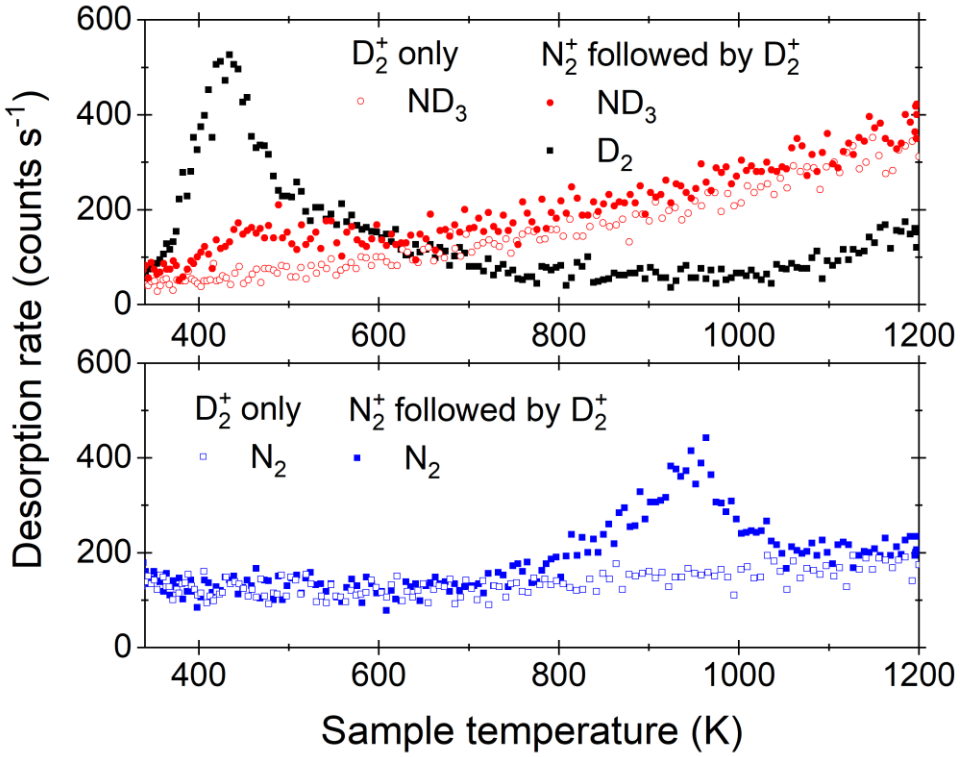

Figure 3. Comparison of raw TPD measurements obtained for two different implantations: open symbols are for a D_2^+ implantation only (red: m/z=20; blue: m/z=14), while solid symbols are for a sequential co-implantation of N_2^+ followed by D_2^+ (black: m/z=4; red: m/z=20; blue: m/z=14). Desorption of ND_3 is visible, between 350 K and 650 K, only during the sequential N_2^+ / D_2^+ implantation. Nitrogen fluence is 1.2×10^{20} N^+ m^{-2} while deuterium fluence is 2.8×10^{19} D^+ m^{-2}.

Figure 3 shows the comparison between two (co-)implantation experiments. Open symbols represent the desorption rates of products at m/z=14 (blue) and m/z=20 (red) after a D ion implantation of 2.8×10^{19} D^+ m^{-2}. Clearly, after D ion implantation there is no peak of desorption for the N_2 product (m/z=14) nor for D_2O or ND_3 products (m/z=20). Solid symbols show the desorption rates of products at m/z=14 (blue) and m/z=20 (red) after a sequential co-implantation of N ions (1.2×10^{20} N^+ m^{-2}) and D ions (2.8×10^{19} D^+ m^{-2}). Now, two additional peaks of desorption are observed, one peak for m/z=14 between 800 K and 1100 K, ascribed to N_2 desorption, and one peak for m/z=20 between 350 K and 650 K. Since the desorption peak for m/z=20 is observed only when both deuterium and nitrogen ions were co-implanted, we infer that the product at m/z=20 must be attributed to ND_3 in our experimental conditions.

Note that ND_3 desorption occurs in conjunction with the D_2 product (black solid symbols in figure 3) while N_2 desorption starts only above 800 K. The separation in temperature of the release of the deuterated products, D_2 and ND_3, from the N_2 product will be exploited in section 3.3. to gain information on the formation mechanism of ND_3 on tungsten.

3.2.2. Quantification of deuterated ammonia production

First, we have compared the production of ND_3 during a TPD ramp from a near-saturated nitrogen layer (fluence of 4.5×10^{20} N^+ m^{-2}, corresponding to three-fourths of a saturated N layer) for different D ion fluence (figure 4, solid green squares). When the deuterium fluence is increased it is found that the production of ND_3 increases up to a maximum production of $3.8\pm0.2\times10^{17}$ ND_3 m^{-2}. This saturation of the deuterated ammonia production is reached for D ion fluence above 1×10^{20} D^+ m^{-2}.

We also compared the production of ND_3 during a TPD ramp at a low and a high D ions fluence for different N-implanted tungsten layers (Figure 4). First, a low D ions fluence of 2.8×10^{19} D^+ m^{-2} was implanted in two different N layers: one at three-fourths of saturation (fluence of 4.5×10^{20} N^+ m^{-2}, solid green square) and one at a fourth of saturation (fluence of 1.2×10^{20} N^+ m^{-2}, blue open circle). For this low D ion fluence, when the nitrogen density is decreased by a factor of 3, it is found that the ND_3 production is decreased by about a factor of 1.5. Thus, near-saturation of the nitrogen layer is necessary to obtain a significantly large ND_3 production even at low D ion fluence. Second, a high D ion fluence of $2\text{-}3\times10^{20}$ D^+ m^{-2} was implanted in two different N layers: one at three-fourths of saturation (fluence of 4.5×10^{20} N^+ m^{-2}, solid green square) and one at saturation of the N layer (fluence of 1.0×10^{21} N^+ m^{-2}, open red triangles). For this higher D ion fluence, when the nitrogen density is near or at the saturation of the layer, there is no change of the ND_3 production which remains at the 3.8×10^{17} ND_3 m^{-2} level. Therefore, once the N layer approaches saturation, the ND_3 production reaches its maximum.

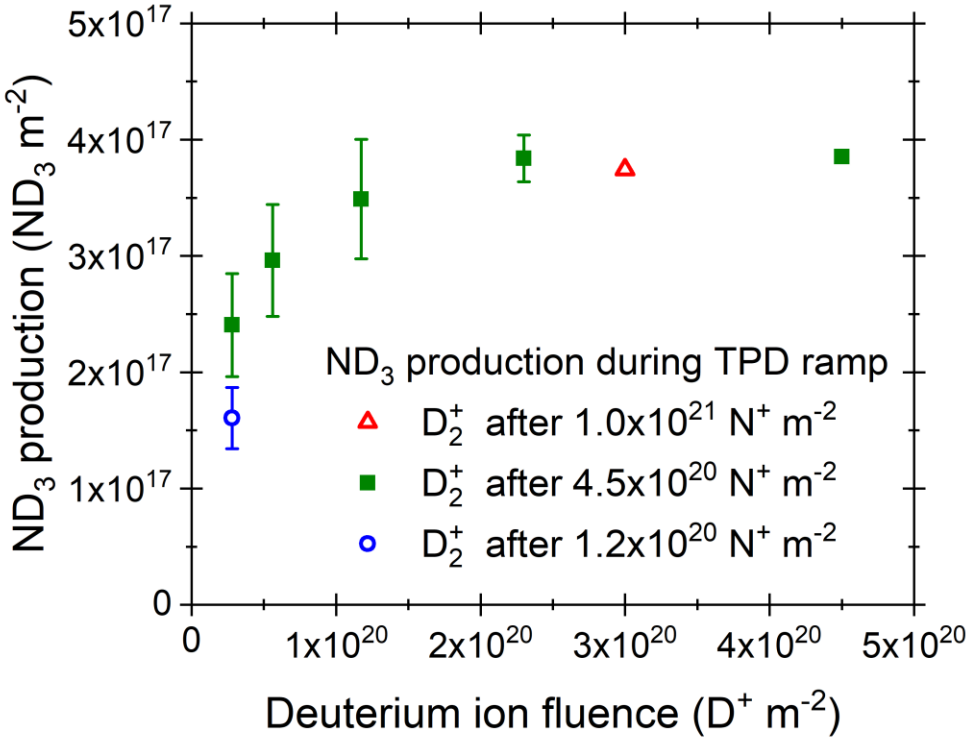

Figure 4. The production of ND_3 as a function of D ion fluence for three different nitrogen layers implanted at 305±4 K. The open blue circle is the result for a fourth of a saturated nitrogen layer ($1.0±0.3×10^{19}$ N m^{-2}). Solid green squares are results for three-fourths of a saturated nitrogen layer ($3.0±0.9×10^{19}$ N m^{-2}). The open red triangle is the result for a saturated nitrogen layer ($4.2±1.1×10^{19}$ N m^{-2}). Data points with error bars (±σ) are the average of at least two replicate experiments.

The maximum production of ND_3 during a TPD ramp contains about $4×10^{17}$ N m^{-2} and $1.2×10^{18}$ D m^{-2}, which are small quantities compared to the content of the near-saturated nitrogen layer ($3.0×10^{19}$ N m^{-2}) and the D ion fluence (> $1×10^{20}$ D^+ m^{-2}). The amount of implanted nitrogen consumed during the TPD ramp that produces ND_3 is very small, i.e. only 1.3 % of the near-saturated N layer. Furthermore, one can note that the amount of deuterium found in ND_3 products is at most 10 % of the tungsten atoms surface density (a tungsten monolayer being about $1.2×10^{19}$ W m^{-2}). This order of magnitude suggests that one may consider the production of ND_3 products over the course of a TPD ramp to happen solely at the tungsten surface. This hypothesis will be tested in section 3.3.

To conclude on the quantitative measurements performed here, we note that for the D fluence investigated presently, and with an implantation temperature of 305±4 K, we did not observe a significant loss of nitrogen in the N-implanted layer upon D implantation. For a fluence of 1.2×10^{20} N^+ m^{-2}, we measured a N retention of $1.0\pm0.3\times10^{19}$ N m^{-2} for N-implantation only versus $1.1\pm0.3\times10^{19}$ N m^{-2} for a N+D sequential co-implantation with 2.8×10^{19} D^+ m^{-2}. For a fluence of 4.5×10^{20} N^+ m^{-2}, we measured a N retention of $3.0\pm1.0\times10^{19}$ N m^{-2} for N-only versus $3.1\pm1.0\times10^{19}$ N m^{-2} for a N+D co-implantation with 1×10^{20} D^+ m^{-2} and, albeit measured only once, we measured a N retention of 3.1×10^{19} N m^{-2} after co-implantation with 4.5×10^{20} D^+ m^{-2}. Thus, considering our uncertainty on N retention measurements and ND_3 production rate, it can be said that N loss in the N-implanted layer during D-co-implantation is less than 30% at room temperature.

3.3. Formation mechanism of deuterated ammonia on tungsten

3.3.1. Bulk or surface-limited?

In the previous section, we found that the saturated amount of ND_3 produced during a TPD ramp was small (3.8×10^{17} ND_3 m^{-2}) relatively to the amount of nitrogen present in the (near-) saturated nitrogen layer ($3\text{-}4\times10^{19}$ N/m^2). These values indicate that only a small fraction of the available nitrogen (1.3% on average) is consumed to produce ND_3 products (desorbing below 650 K), the rest producing N_2 molecules (desorbing above 800 K). This result could be interpreted in two ways. On the one hand, in the hypothesis where ND_3 precursors could be formed within the nitrogen layer, it would mean that the process of deuterium binding to nitrogen within the bulk, or the process of diffusion of ND_3 precursors, would be inefficient. On the other hand, if ND_3 precursors can only be formed at the tungsten surface, it would mean that the nitrogen concentration in the surface layer would be small or that a competition between ND_3 production and D_2 production occurs. At first glance, the last two explanations of a surface-assisted production of ND_3 sound the most plausible. Furthermore, we have shown in section 3.2.2 that the amount of deuterium found in ND_3 products is well below the tungsten atoms surface density (about 10%) and thus does not contradict the surface-production hypothesis. Therefore, in the following we will investigate this surface-production hypothesis.

Since N_2 desorption occurs after D_2 and ND_3 desorption, with no overlap in desorption temperature range, we were able to test the surface-production hypothesis by using interrupted TPD ramp with the following cycles experiments. For the first cycle, we

performed a sequential co-implantation of N_2^+ / D_2^+ followed by a TPD ramp interrupted at 750 K, i.e. not desorbing the N implanted layer. For the second and subsequent cycles, we realized additional D_2^+ implantations at *301±1 K* (same fluence as the first cycle) followed by a TPD ramp interrupted again at 750 K to keep the N implanted layer in W. Cycles experiments were performed for a three-fourths saturated N layer (fluence of 4.5×10^{20} N^+ m^{-2}, green solid squares in figure 5) and a saturated N layer (fluence of 1.0×10^{21} N^+ m^{-2}, red open triangles in figure 5) with D ion fluence of 2.3×10^{21} D^+ m^{-2} and 3.0×10^{21} D^+ m^{-2}, respectively.

Figure 5 presents the results of these cycles experiments and reveals that more than the initial 3.8×10^{17} ND_3 m^{-2} can be produced from a (near-) saturated N layer. In particular, a common behaviour is observed for the two investigated N/D sets of fluences: the ND_3 production rate decreases monotonously with the cycle number. Using a linear fit for these decays, we find that an absence of ND_3 production should be observed after 4 and 5 cycles of implantation/interrupted TPD for the near-saturated N layer and the saturated N layer, respectively. Summing up the total quantity of ND_3 produced within these cycles for these N layers, we estimate that no more than 1×10^{18} ND_3 m^{-2} could be produced. Using a more conservative estimate for the decay of ND_3 production with increasing the cycle number, i.e. an exponential decay, we found that for the saturated N layer there should not be any detectable ND_3 production after 6 cycles of implantation/interrupted TPD. In this case the total quantity of ND_3 produced would be $< 2\times10^{18}$ ND_3 m^{-2}. Thus, less than 5% of the total nitrogen present in the saturated N layer can be consumed during these cycles of D implantation and thermal release up to 750 K. This striking result demonstrates that not all nitrogen in the N layer is mobilized for ND_3 production, even with a temperature sweep to 750 K, consistent with a negligible N diffusion below 800 K [11], and thus it points towards a surface-limited mechanism for ND_3 production on tungsten. We stress that the exponential decay of ND_3 production with cycle number cannot be explained solely by a hypothetical high N loss of the N-implanted layer upon D co-implantation. Such implantation-induced N loss of ca 30% (defined by our detection uncertainties) would diminish ND_3 production to 2.6×10^{17} ND_3 m^{-2} in the second cycle, when we measured only about 1.9×10^{17} ND_3 m^{-2} (Figure 5). Thus, the ND_3 diminished production with increasing D implantation/TPD cycling is truly, at least in part, the results of a loss of N due to the production of ND_3 from the accessible reservoir, i.e. the N at the surface.

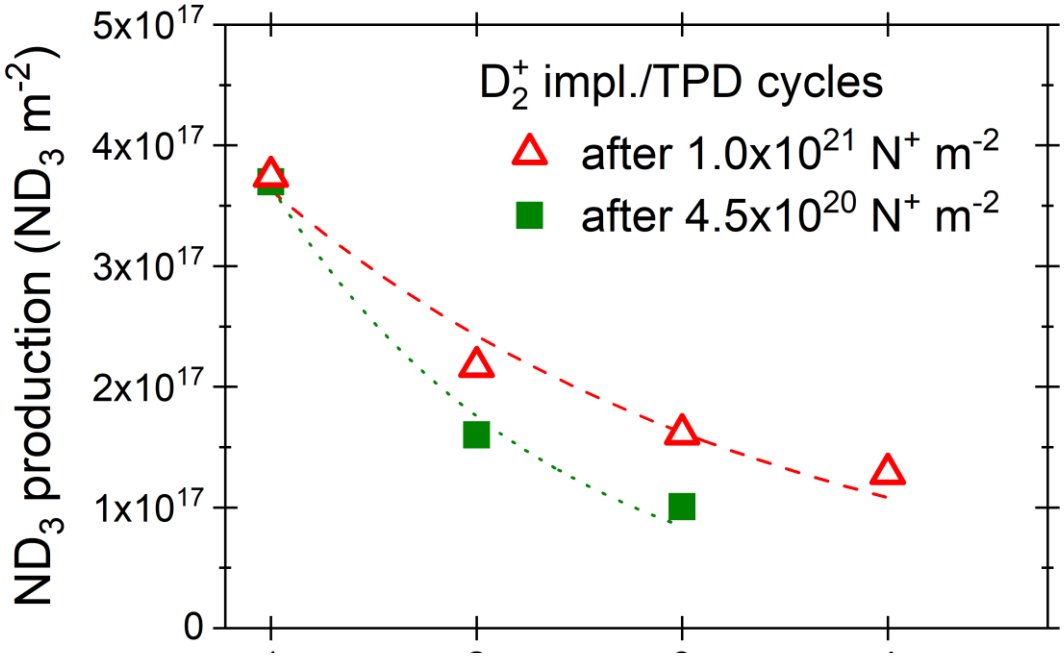

Figure 5. The production of ND_3 in near-saturated (green solid squares) and saturated (red open triangles) nitrogen layers in W obtained by successive cycles of D_2^+ implantation at 301±1 K (2.3×10^{20} D^+ m^{-2} per cycle for green solid squares and 3.0×10^{20} D^+ m^{-2} per cycle for red open triangles) and TPD up to 750 K (i.e. below N desorption temperature). The exponential decays of ND_3 production with cycle number are shown with dashed and dotted lines.

Assuming that for a saturated N layer on W at most 2×10^{18} ND_3 m^{-2} can be produced and that the consumed nitrogen is only the one at the surface (with an atomic W surface density of 1.2×10^{19} m^{-2}), we can estimate that about 17% of the surface atoms at the N saturated W samples are nitrogen atoms. This result is consistent with SDTrimSP calculations performed by Meisl *et al.* [10], whom estimate the nitrogen concentration in the first layer of tungsten to be on the order of 20 % (2.4×10^{18} N m^{-2}) for similar implantation conditions (320 eV/N at a 40° incidence angle). Again, this quantity of ammonia (2×10^{18} ND_3 m^{-2}) is an upper limit valid only for a saturated N-implanted layer created at room temperature. Smaller ammonia production is expected for N implantation occurring above room temperature given the decreased N density at saturation observed by Plank *et al.* when increasing the W temperature during N implantation.

3.3.2. Formation of ammonia precursors on the tungsten surface

We interpreted the observation of a limited production of ND_3 on N-implanted tungsten as a signature of ND_3 production occurring at the surface. To confirm this interpretation, we performed vibrational spectroscopy of surface species on our polycrystalline W sample using HREELS. A beam of monochromatic and low energy electrons was scattered on the W sample and the energy loss of these electrons after their interactions with the surface was recorded with an electrostatic cylindrical analyser. The electrons energy losses are due to the excitation of vibrational modes of adsorbates that can thus be identified as shown in figure 6.

A 1100 K annealed W sample (black open circle) does not show any vibrational signature in the 0.20 – 0.50 eV loss range typical for hydrogen isotopes bound to C, N and O adsorbates. W-O and W-C vibrations are however visible in the 0.00 – 0.20 eV range (not shown) consistent with the presence of C and O natural impurities in high purity W samples annealed below 2200 K.

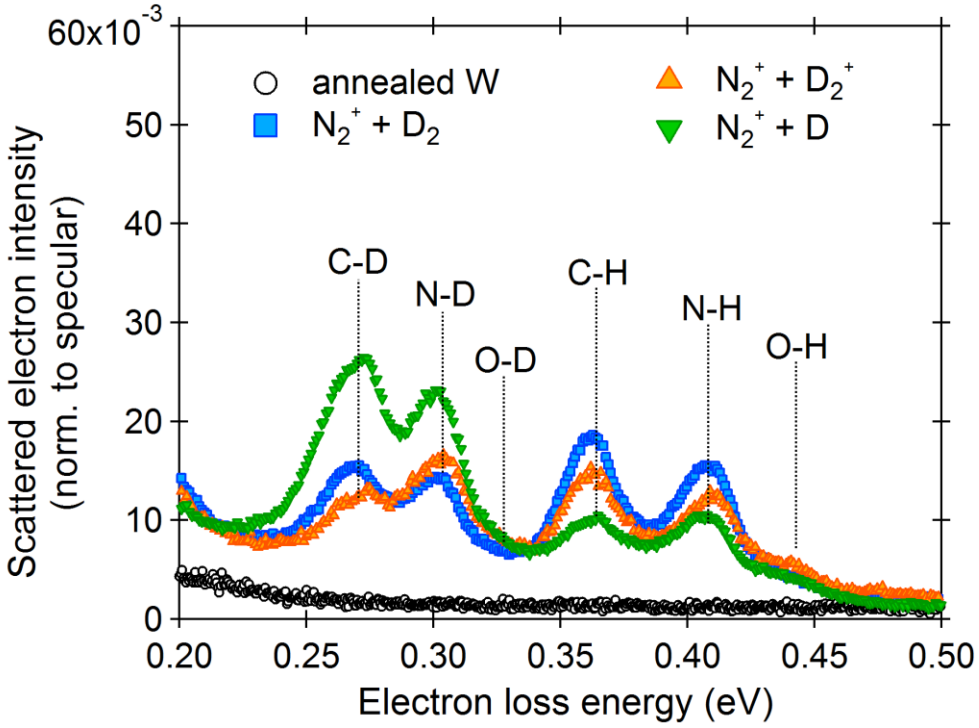

Figure 6. Vibrational spectra of the surface of tungsten after various sequential exposure to nitrogen and deuterium species at room temperature. Between each spectra the sample is annealed to 1100 K (black circles). Blue squares: nitrogen ions (250 eV/N) followed by thermal deuterium molecules (0.04 eV/D_2). Orange triangles: nitrogen ions (250 eV/N) followed by deuterium ions (250 eV/D). Green triangles: nitrogen ions (250eV/N) followed by deuterium atoms (0.25 eV/D).

Upon sequential co-implantation of N and D ions at 250 eV per nucleus (orange solid triangle), several vibrational signatures typical of hydrogen isotopes bound to natural (C and O) and implanted (N) impurities are observed. The presence of N-D surface vibrations evidences the presence of ND_3 precursor at the surface of N-implanted W. The O-D vibrational signature is barely seen because of the presence of a strong C-H signature. H bound to C, O and N impurities are also detected with similar intensities indeed, even though 99.8% D_2 was used as a gas feed. This surprising result suggests that the N-implanted W surface catalyzes the dissociation of the residual H_2 present in the UHV chamber.

We demonstrate the catalyzing effect of N on W on the dissociative adsorption of H_2/D_2 neutral molecules by comparing the HREELS spectra of pristine W exposed to H_2/D_2 (Figure 6, black open circle), where there is no vibrational signature of H/D, with the HREELS spectra of N-implanted W exposed to H_2/D_2 (blue solid square) where C-D and N-D signatures are observed together with C-H, N-H and O-H signatures. Note that when we performed the implantation of solely N ions, we registered also the C-H, N-H and O-H signatures because the residual H_2 in the vacuum chamber readily dissociate and bind on N-implanted W surfaces (but not on pristine W).

In figure 7, we confirm the catalysing effect of N-implanted W surfaces regarding molecular deuterium dissociation by comparing thermo-desorption of annealed W exposed to D_2 molecules (with the same amount of pressure×time than when performing D ion implantation with 2.8×10^{19} D^+ m^{-2}) versus a N-implanted W layer (1.2×10^{20} N^+ m^{-2}, a fourth of saturation) exposed to D_2 molecules with similar conditions. Obviously, the N-implanted W sample exposed to D_2 molecules desorbed much more deuterium during the TPD (blue solid squares) than the annealed pristine W sample exposed to D_2 (black solid circles). The deuterium release due to the catalysed dissociation of D_2 on N-implanted W layers is 1.6×10^{17} D m^{-2} which is on par with the expected N density at the surface at a fourth of saturation of the nitrogen layer, i.e. ~6×10^{17} N m^{-2} according to the reduction of the N1s/W4f XPS signal observed by Meisl *et al.* [10] in their fluence dependence study, and consistent with the observation of N-D surface vibrational signature in figure 6 (blue squares). This 1.6×10^{17} D m^{-2} due to D_2 catalysed dissociative chemisorption at the surface of N-implanted W is to be compared with the 1.6×10^{17} ND_3 m^{-2} obtained when D_2^+ co-implantation is performed in similar time×pressure conditions (blue open circle in figure 4) and the concurrent release of

$2.4\pm0.6\times10^{18}$ D m^{-2} from the bulk (not shown). These results highlight that ND_3 production on W is in competition with the production of D_2 molecules (formed from D at the surface and from the bulk) and that ND_3 production is a minority channel when using D/N ions sequential co-implantation.

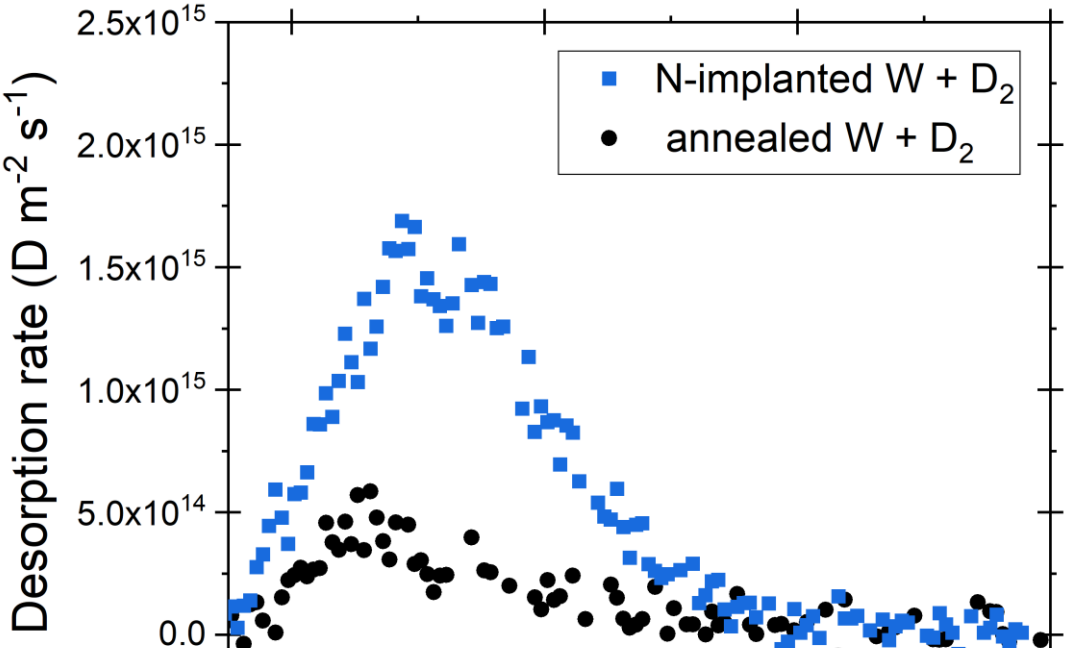

Figure 7. Comparison of TPD measurements after D_2 molecular exposure on: (black solid circles) annealed W, the observed deuterium release originates from the oven assembly; (blue solid squares) N-implanted W, the increased desorption of deuterium evidences the catalysing effect of the presence of nitrogen on the W surface for deuterium molecule dissociative adsorption.

Finally, we explored the effect of deuterium pre-dissociation onto the generation of ND_3 precursors at the surface by exposing the N-implanted W sample to a beam of D^0 atoms (green solid triangles in figure 6). We observed an overall reduction of H bound surface species and a strong increase in D bound surface species, including N-D precursors. The enhanced production of D bound species is presumably due to the efficient abstraction reaction between gas phase impinging deuterium atoms and surface H bound species. Thus, this surface-localized type of reaction involving a radical favour the creation of ND_3 precursors and one can expect that it could favour the production of ammonia by a chemical etching mechanism such as the one observed by Küppers and co-workers on platinum for deuterium atoms impinging on oxygen and sulphur adsorbates on metals [34, 35] or on

amorphous carbon [36]. Such reactions leading to the production of ammonia on tungsten will be the subject of future studies in our laboratory.

4. SUMMARY AND PERSPECTIVES

First, we quantified the retention of nitrogen in tungsten and characterized its desorption by temperature programmed desorption. Saturation of the nitrogen layer has been observed at room temperature while a zero-order desorption kinetics is measured between 800 K and 1100 K. These results are consistent with the W-N phase diagram proposed by Schmid et al. [31] and previous works performed at different kinetic energies and incidence angles [10–12].

Second, we quantified the ND_3 production from co-implanted N and D ions in W for different densities of the nitrogen layer. We observed that the production of ND_3 molecules on W occurs in a surface temperature range (350 – 650 K) concomitant with D_2 (and HD) desorption and separately from N_2 desorption. We showed that significant ND_3 production can be obtained with N-implanted tungsten materials only if a near-saturated N layer is present. Then, we demonstrated that the quantity of ND_3 produced from a near-saturated N layer is limited by the N density at the outermost layer of the surface of W. Lastly, we evidenced the presence of ND_3 precursor at the surface of N-implanted W thanks to vibrational spectroscopy and showed that the presence of N at the surface of W catalyses the dissociative adsorption of D_2 molecules.

Finally, these results should be useful to better model and estimate ammonia production in tokamaks operating N-seeded plasma discharge with W PFCs. In addition to offer an understanding of the surface-limited mechanism behind the production of ammonia on W, the quantitative estimate of ammonia production provided here could be combined with the previously reported effect of W temperature on the creation of a N layer [11] to define an upper limit for the production of ammonia from W PFCs as a function of their temperature. The temperature and N surface exposure conditions necessary for significant ammonia production on W materials being clarified, one should analyze past and future experiments in WEST and ASDEX Upgrade with this dual conditions in mind.

Acknowledgments

The project leading to this publication has received funding from Excellence Initiative of Aix-Marseille University - A*MIDEX, a French Investissements d'Avenir programme. We thank the financial support of the French Federation for Magnetic Fusion Studies (FR-FCM). This work has been carried out within the framework of the EUROfusion Consortium and has received funding from the Euratom research and training programme 2014-2018 and 2019-2020 under grant agreement No 633053. The views and opinions expressed herein do not necessarily reflect those of the European Commission. Work performed under EUROfusion WP PFC. The views and opinions expressed herein do not necessarily reflect those of the ITER Organization. ITER is the Nuclear Facility INB no. 174. This paper applies new physics analysis related to tritiated ammonia formation, which is not yet incorporated into the ITER technical baseline. The nuclear operator is not constrained by the results presented here.

References

[1] DE TEMMERMAN, G., HIRAI, T., PITTS, R.A., The influence of plasma-surface interaction on the performance of tungsten at the ITER divertor vertical targets, Plasma Phys. Control. Fusion **60** 4 (2018) 044018.
[2] KALLENBACH, A. et al., Divertor power load feedback with nitrogen seeding in ASDEX Upgrade, Plasma Phys. Control. Fusion **52** 5 (2010) 055002.
[3] SCHWEINZER, J. et al., Confinement of `improved H-modes' in the all-tungsten ASDEX Upgrade with nitrogen seeding, Nucl. Fusion **51** 11 (2011) 113003.
[4] GIROUD, C. et al., Impact of nitrogen seeding on confinement and power load control of a high-triangularity JET ELMy H-mode plasma with a metal wall, Nucl. Fusion **53** 11 (2013) 113025.
[5] NEUWIRTH, D., ROHDE, V., SCHWARZ-SELINGER, T., ASDEX UPGRADE TEAM, Formation of ammonia during nitrogen-seeded discharges at ASDEX Upgrade, Plasma Phys. Control. Fusion **54** 8 (2012) 085008.
[6] OBERKOFLER, M. et al., First nitrogen-seeding experiments in JET with the ITER-like Wall, J. Nucl. Mater. **438** (2013) S258.
[7] DRENIK, A. et al., Evolution of nitrogen concentration and ammonia production in N2-seeded H-mode discharges at ASDEX Upgrade, Nucl. Fusion **59** 4 (2019) 046010.
[8] MINISSALE, M. et al., Sticking Probability of Ammonia Molecules on Tungsten and 316L Stainless Steel Surfaces, J. Phys. Chem. C **124** 32 (2020) 17566.
[9] LOARER, T. et al., Long discharges in steady state with D2 and N2 on the actively cooled tungsten upper divertor in WEST, Nucl. Fusion **60** 12 (2020) 126046.
[10] MEISL, G. et al., Implantation and erosion of nitrogen in tungsten, New J. Phys. **16** 9 (2014) 093018.
[11] PLANK, U., MEISL, G., TOUSSAINT, U. von, HÖSCHEN, T., JACOB, W., Study of the temperature-dependent nitrogen retention in tungsten surfaces using X-ray photoelectron spectroscopy, Nucl. Mater. Energy **17** (2018) 48.
[12] OGORODNIKOVA, O.V. et al., Effect of nitrogen seeding into deuterium plasma on deuterium retention in tungsten, Phys. Scr. **T145** (2011) 014034.

[13] GAO, L. et al., Interaction of deuterium plasma with sputter-deposited tungsten nitride films, Nucl. Fusion **56** 1 (2016) 016004.
[14] DE CASTRO, A., ALEGRE, D., TABARÉS, F.L., Ammonia formation in N2/H2 plasmas on ITER-relevant plasma facing materials: Surface temperature and N2 plasma content effects, J. Nucl. Mater. **463** (2015) 676.
[15] DE CASTRO, A., TABARÉS, F.L., Role of nitrogen inventory and ion enhanced N-H recombination in the ammonia formation on tungsten walls. A DC glow discharge study, Vacuum **151** (2018) 66.
[16] LAGUARDIA, L. et al., Influence of He and Ar injection on ammonia production in N2/D2 plasma in the medium flux GyM device, Nucl. Mater. Energy **12** (2017) 261.
[17] YAALA, M.B. et al., Plasma-assisted catalytic formation of ammonia in N2–H2 plasma on a tungsten surface, Phys. Chem. Chem. Phys. (2019).
[18] YAALA, M.B. et al., Plasma-activated catalytic formation of ammonia from N2–H2: influence of temperature and noble gas addition, Nucl. Fusion **60** 1 (2019) 016026.
[19] KALININ, G. et al., ITER R&D: Vacuum Vessel and In-vessel Components: Materials Development and Test, Fusion Eng. Des. **55** 2–3 (2001) 231.
[20] BISSON, R. et al., Dynamic fuel retention in tokamak wall materials: An in situ laboratory study of deuterium release from polycrystalline tungsten at room temperature, J. Nucl. Mater. **467** 1 (2015) 432.
[21] HODILLE, E.A. et al., Retention and release of hydrogen isotopes in tungsten plasma-facing components: the role of grain boundaries and the native oxide layer from a joint experiment-simulation integrated approach, Nucl. Fusion **57** 7 (2017) 076019.
[22] GHIORGHIU, F. et al., Comparison of dynamic deuterium retention in single-crystal and poly-crystals of tungsten: The role of natural defects, Nucl. Instrum. Methods Phys. Res. Sect. B Beam Interact. Mater. At. **461** (2019) 159.
[23] ZIEGLER, J.F., ZIEGLER, M.D., BIERSACK, J.P., SRIM – The stopping and range of ions in matter (2010), Nucl. Instrum. Methods Phys. Res. Sect. B Beam Interact. Mater. At. **268** 11–12 (2010) 1818.
[24] KIM, Y.-K. et al., Electron-Impact Cross Sections for Ionization and Excitation Database, text NIST Standard Reference Database 107, (2004).
[25] REJOUB, R., LINDSAY, B.G., STEBBINGS, R.F., Electron-impact ionization of NH3 and ND3, J. Chem. Phys. **115** 11 (2001) 5053.
[26] BOCQUET, F.C., BISSON, R., THEMLIN, J.-M., LAYET, J.-M., ANGOT, T., Reversible hydrogenation of deuterium-intercalated quasi-free-standing graphene on SiC(0001), Phys. Rev. B **85** 20 (2012) 201401.
[27] TSCHERSICH, K.G., Intensity of a source of atomic hydrogen based on a hot capillary, J. Appl. Phys. **87** 5 (2000) 2565.
[28] BISSON, R., PHILIPPE, L., CHÂTELET, M., Angle-resolved study of hydrogen abstraction on Si(1 0 0) and Si(1 1 1): Evidence for non-activated pathways, Surf. Sci. **600** 19 (2006) 4454.
[29] SMITH, R.S., MAY, R.A., KAY, B.D., Desorption Kinetics of Ar, Kr, Xe, N_2, O_2, CO, Methane, Ethane, and Propane from Graphene and Amorphous Solid Water Surfaces, J. Phys. Chem. B **120** 8 (2016) 1979.
[30] KING, D.A., MADEY, T.E., YATES, J.T., Interaction of Oxygen with Polycrystalline Tungsten. II. Corrosive Oxidation, J. Chem. Phys. **55** 7 (1971) 3247.
[31] SCHMID, K. et al., Interaction of nitrogen plasmas with tungsten, Nucl. Fusion **50** 2 (2010) 025006.
[32] VENABLES, J.A., BIENFAIT, M., On the reaction order in thermal desorption spectroscopy, Surf. Sci. **61** 2 (1976) 667.

[33] MATEUS, R. et al., Thermal and chemical stability of the β-W2N nitride phase, Nucl. Mater. Energy **12** (2017) 462.
[34] BIENER, J., LANG, E., LUTTERLOH, C., KÜPPERS, J., Reactions of gas-phase H atoms with atomically and molecularly adsorbed oxygen on Pt(111), J Chem Phys **116** 7 (2002) 3063.
[35] GÜTTLER, A., KOLOVOS-VELLIANITIS, D., ZECHO, T., KÜPPERS, J., Abstraction of sulfur from Pt(1 1 1) surfaces with thermal H atoms toward adsorbed and gaseous H2S, Surf. Sci. **516** 3 (2002) 219.
[36] ZECHO, T., BRANDNER, B.D., BIENER, J., KÜPPERS, J., Hydrogen-Induced Chemical Erosion of a-C:H Thin Films: Product Distribution and Temperature Dependence, J. Phys. Chem. B **105** 26 (2001) 6194.